AIP | Applied Physics Letters

Room temperature large-area nanoimprinting for broadband biomimetic antireflection surfaces

Hakan Deniz, Tural Khudiyev, Fatih Buyukserin, and Mehmet Bayindir

Citation: Appl. Phys. Lett. **99**, 183107 (2011); doi: 10.1063/1.3657766
View online: http://dx.doi.org/10.1063/1.3657766
View Table of Contents: http://apl.aip.org/resource/1/APPLAB/v99/i18
Published by the American Institute of Physics.

Related Articles

Monolithic polymer microlens arrays with antireflective nanostructures
Appl. Phys. Lett. 101, 203102 (2012)

Fourier transform infrared absorption spectroscopy characterization of gaseous atmospheric pressure plasmas with 2 mm spatial resolution
Rev. Sci. Instrum. 83, 103508 (2012)

Antireflective ZnSnO/Ag bilayer-based transparent source and drain electrodes for transparent thin film transistors
Appl. Phys. Lett. 100, 263505 (2012)

Ultrasonic evaluation of early damage of a coating by using second-harmonic generation technique
J. Appl. Phys. 111, 124902 (2012)

Electrochromic switchable mirror glass with controllable reflectance
Appl. Phys. Lett. 100, 091906 (2012)

Additional information on Appl. Phys. Lett.

Journal Homepage: http://apl.aip.org/
Journal Information: http://apl.aip.org/about/about_the_journal
Top downloads: http://apl.aip.org/features/most_downloaded
Information for Authors: http://apl.aip.org/authors

ADVERTISEMENT

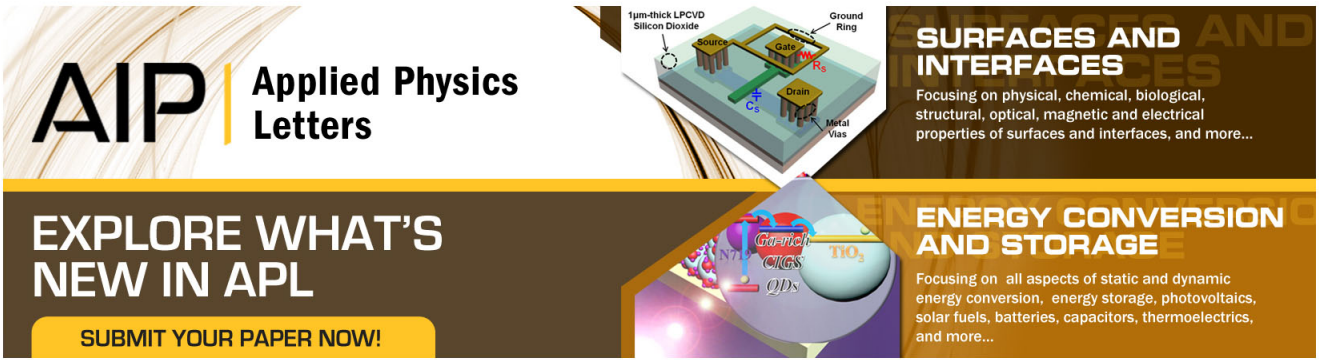

Room temperature large-area nanoimprinting for broadband biomimetic antireflection surfaces

Hakan Deniz,[1,2] Tural Khudiyev,[1,2] Fatih Buyukserin,[3] and Mehmet Bayindir[1,2,4,a)]
[1]*UNAM-National Nanotechnology Research Center, Bilkent University, 06800 Ankara, Turkey*
[2]*Institute of Materials Science and Nanotechnology, Bilkent University, 06800 Ankara, Turkey*
[3]*Department of Biomedical Engineering, TOBB University, 06560 Ankara, Turkey*
[4]*Department of Physics, Bilkent University, 06800 Ankara, Turkey*

(Received 28 July 2011; accepted 12 October 2011; published online 2 November 2011)

Ordered arrays of subwavelength hydrogen silsesquioxane (HSQ) nanorods on glass substrates are fabricated using room temperature nanoimprint lithography and anodized aluminum oxide membranes. Moth-eye type nanorod arrays exhibited superior omnidirectional antireflection characteristics in visible wavelengths. The ellipsometric measurements revealed that average specular reflection is remaining below 1% up to 55° incidence angles. Transmission measurements at normal incidence resulted in significant increase in transmitted light intensity with respect to plain glass. Simulations showed that up to 99% transmission could be obtained from double sided tapered HSQ nanorod arrays on HSQ thin film and glass substrates. Achieving large-area, broadband and omnidirectional antireflective surfaces on glass pave the way for applications including photovoltaics. © *2011 American Institute of Physics*. [doi:10.1063/1.3657766]

Reflection is an unwanted optical effect that arises when the light travels from one medium into another with different optical properties. To reduce reflection from surfaces and improve transmission, most optical components are coated with thin films called antireflection (AR) coatings. Most common AR coatings are single/multi-layer dielectric thin films which exploit destructive interference of light rays reflected from the interfaces to reduce the intensity of the reflected light. However, they provide antireflection properties only for a limited range of incidence angles and spectral wavelengths. To overcome the shortcomings of conventional AR coatings, the graded refractive index layers method or the antireflective structure (ARS) method can be effectively utilized to reduce the reflection from the surfaces.[1–3]

The ARS is particularly inspired by nature, found on the compound eyes of nocturnal insects, such as moth and some butterflies.[4,5] The ARS, sometimes also called as moth-eye antireflection coatings, comprises of non-close packed nipple arrays with sub-wavelength dimensions. These arrays on the cornea of moth eyes with their tapered profiles exhibit a gradual change between the refractive index of surrounding air and corneal surface and decrease the reflectance by optical impedance matching at the interfaces. Demonstrations of moth-eye AR coatings have proven to be a promising and efficient way for producing broadband and omni-directional AR properties for solar cell applications, displays, and lenses.[6–9] The other common method used frequently in order to obtain antireflective coating is nanostructuring fused silica surface by plasma etching through a well-defined mask.[10,11]

In this work, we report the fabrication of biomimetic nanorod arrays on glass substrates using a well-defined molecular precursor, hydrogen silsesquioxane (HSQ) and anodized aluminum oxide (AAO) membranes by means of nanoimprint lithography (NIL). AAO membranes as template offer high density long-range ordered porous architecture with hexagonal symmetry and flexibility to tailor the shape, periodicity, and aspect ratio for the production of nanostructures for antireflection purposes.[12,13] Other technologically important template technique is nanoimprint lithography, which has been shown to be a simple and low cost method with high resolution and throughput in fabricating nano-scale antireflection coatings.[14] We chose HSQ as a resist material because it can be used in room temperature nanoimprinting without any further treatment, producing features with very high resolution linewidth.

NIL was performed with the direct use of free standing AAO membranes as a mold instead of replicating and transferring porous structure onto some other substrate, such as silicon or silica. AAO membranes were prepared as described in a previous report.[15] They have a pore size of 100 nm and a periodicity of 130 nm (Fig. 1(a)). Major steps in the fabrication of HSQ nanorod arrays are illustrated in Fig. 1(b). In first step, HSQ resin was spin-coated on glass substrates at different speeds to adjust the final film thicknesses. After spin-coating, the samples were placed on hot plate at 50 °C for 20 min for the solvent to evaporate. Pieces of AAO membranes were placed on mica substrates with their barrier layer side facing down and their polished side facing up. In second step, HSQ films and AAO membranes were brought into a conformal contact and a pressure of about 2000-2500 psi was applied to replicate the negative image of porous structure of AAO membranes onto HSQ resist. After NIL was performed, AAO membranes are stuck onto HSQ film and come off from mica substrates easily due to large-scale roughness of barrier layer side of AAO membranes. Samples were later cured at 400 °C in rough vacuum conditions for 1 h. Barrier layer of AAO membranes were plasma etched with Ar in inductively coupled plasma (ICP) etch system so that subsequent wet etch will dissolve AAO membrane without any contaminants left. This process ensured that the rough barrier side was etched away quickly without damaging nanorods underneath. Remaining AAO

a)Electronic mail: bayindir@nano.org.tr.

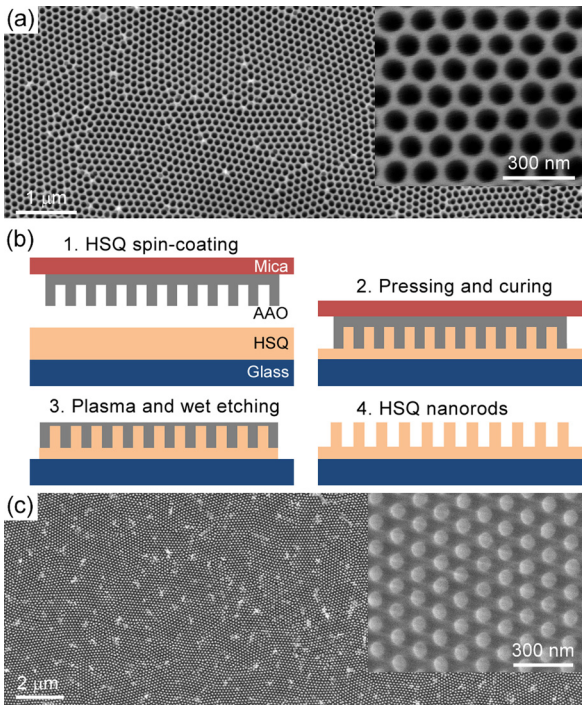

FIG. 1. (Color online) (a) SEM image of AAO membranes showing porous architecture over a large area before used in NIL (inset is high magnification image of same membrane showing hexagonal ordering and pore size). (b) Schematic illustrations describing fabrication steps of HSQ ordered nanorod arrays. (c) SEM micrograph of HSQ nanorod arrays (inset shows high magnification image of same ordered arrays).

membrane was dissolved in phosphoric acid (25% vol.) overnight without any structural damage to HSQ nanorods. Samples were finally dried in a critical point drier (CPD) to prevent the collapse of structures and stiction of nanorods to each other. When samples were cured, AAO membrane on top of imprinted nanorod structures prevented remaining solvent left in HSQ from being evaporated out of the film, and this could be seen as thin semi-transparent porous-like structures on top of the nanorods. This was cleaned away with CF_4 plasma etch in ICP by carefully monitoring the etch time in order not to etch away nanorods. Large area SEM image in Fig. 1(c) shows that high density ordered periodic nanorod arrays can be produced in this way. High resolution SEM image at the inset shows the well-ordered structure of nanorods having a lattice constant of 130 nm with hexagonal symmetry. They have a diameter of about 80 nm with heights varying from 200 nm to 400 nm. Final diameter and height of these nanorod arrays can be further tuned in the final CF_4 plasma cleaning step in ICP by adjusting the etch time.

Spectroscopic ellipsometry was employed to measure the intensity of the reflected light from HSQ nanorod arrays on glass surface at oblique incidences. Nano-textured glass surface was illuminated with a collimated beam (~1 mm in diameter) using the Xenon light source of spectroscopic ellipsometer and coherent specular reflectance (including TE and TM polarized reflected light) was measured in visible spectrum (400–800 nm) as the incidence angle changed from 15° to 65° after baseline correction for the light source was done. Figs. 2(a) and 2(b) show total specular reflectance observed from thin film HSQ and nano-patterned HSQ, respectively. At incidence angles close to normal, HSQ thin

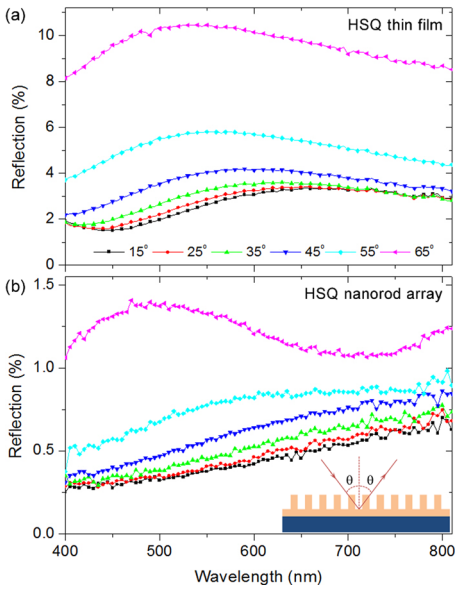

FIG. 2. (Color online) (a) Ellipsometric reflectance measurements acquired at oblique incidences (15°-65°) from HSQ thin film and (b) reflectance curves obtained from ordered HSQ nanorod arrays on the same glass sample at the same incidence angles. Specular reflection from HSQ nanorod surface is below 1% for all visible region up to 55° incidence angles.

film coated glass performs better than plain glass in reducing reflection, but HSQ nanorod arrays surpass both plain glass and HSQ coated glass in performance over a large range of incidence angles (up to 70°). Average specular reflection is less than 1% even at 55° incidence angle. Another interesting feature of these nanorod arrays is their selectivity to TE/TM polarization of incoming light. Average intensity of TM polarized reflected light is almost an order of magnitude smaller than that of TE polarized reflected light. At 60° incidence angle which is very close to Brewster's angle for bare glass (~57°), the intensity difference between TM and TE polarized reflected light becomes as much as 15 fold.

Transmission measurements were performed using a UV-VIS spectrophotometer at normal incidence. Fig. 3(a) shows percent transmission obtained from HSQ nanorod

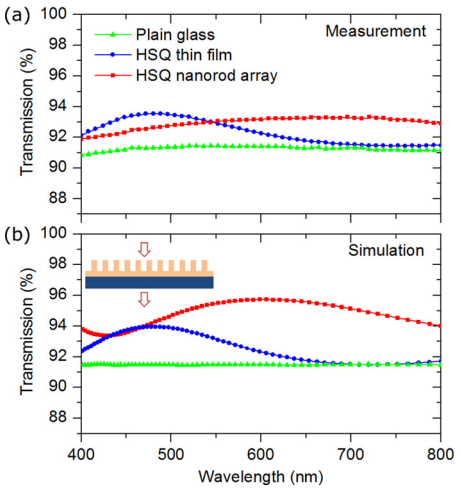

FIG. 3. (Color online) (a) Experimental transmission curves at normal incidence obtained from HSQ nanorod arrays, HSQ thin film, and bare glass substrate. (b) Simulated transmission obtained using approximately the same nanorod height and film thickness as in experimental case. We used n = 1.52 and n = 1.41 for the refractive indices of glass and HSQ, respectively, in simulations.

arrays together with those of HSQ thin film and plain glass for comparison. HSQ thin film data show basic thin film interference, reaching maximum transmission at around the wavelength of 475 nm. Although HSQ nanorod arrays and HSQ thin film on same glass substrate have similar effective thickness on average, nanorod arrays surpass thin film in performance due to its broadband transmission characteristics, except for the wavelengths below 550 nm where thin film transmission is above that of nanorod arrays. Fig. 3(b) shows calculated transmission at normal incidence using finite difference time domain (FDTD) method for systems similar to the ones investigated experimentally above. Measured transmission of nanorod arrays remains below that of simulated one although they have similar transmission behavior. This small discrepancy may arise from the error in measurement of HSQ film thickness, height, and diameter of nanorods, lattice constant, and surface roughness. Simulations indicate that the average tranmission is decreasing as we increase the incidence angle of the light. In our simulations, it is observed that incident Gaussian beam is distorted for reflected and transmitted beams.

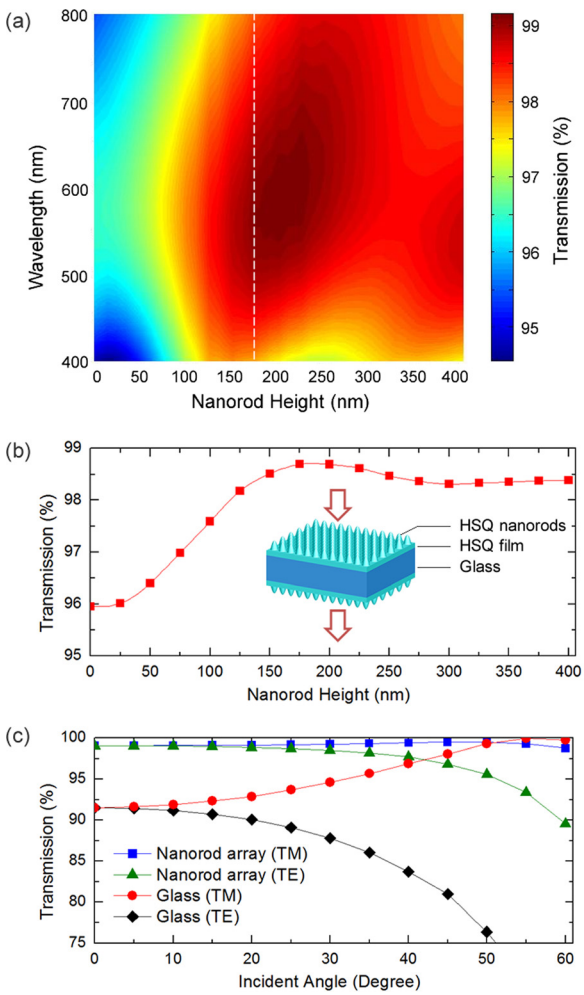

FIG. 4. (Color online) (a) Two-dimensional plot for transmission through HSQ tapered nanorod array on both sides of a glass substrate as a function of nanorod height and wavelength of the light. The vertical dashed line corresponds to the optimum height of nanorods (175 nm). (b) Calculated average transmission as a function of nanorod height for array structures on both sides of glass substrate. (c) Polarization dependent transmission as a function of incidence angle for tapered nanorod array/thin film system at the wavelength of 550 nm.

To optimize this replication procedure further, we have run FDTD simulations to understand the effects of geometry of nanorod arrays. Tapered nanorod arrays can be considered to have a more realistic geometry for biomimicry of moth-eye antireflective structures. 2D map of optimization process is shown for such structures in Fig. 4(a). We defined hexagonally distributed tapered HSQ nanorod arrays on front and back side of glass that has a coverage of 100 nm thin film of HSQ underneath rod arrays (structure shown in inset of Fig. 4(b)). Maximum overall transmission and flat transmission could be obtained when the height of nanorods is 175 nm (dashed line). Same fact is also observable from Fig. 4(b). This type of rod arrays with 100 nm thin film yields up to 98.7% of average transmission in the visible spectrum. Simulations revealed that utilizing this double sided thin film and tapered rod arrays together results in interesting angle-dependent transmission properties. In TE/TM polarizations, we still remain above 90% transmission when incident angle is up to 60°.

In conclusion, biomimetic large-area antireflective surfaces have been fabricated by simple room temperature nanoimprinting scheme using a well-known inorganic resist, without requiring any preparation of special molds. The manufactured nanorod arrays have manifested superior omnidirectional antireflection behavior (up to 70°) with an average reflectance staying below 2% in the visible spectrum (400–800 nm). Transmission characteristic and antireflection behavior of arrays can be improved further by making the geometrical profile of HSQ nanostructures tapered instead of cylindrical and tuning the dimensions as FDTD simulations revealed. These biomimetic surfaces can be of vital technological importance in reducing the reflection of optical components. In future, functional nanorod arrays with self-cleaning and hydrophobic properties can be fabricated by embedding TiO_2/ZnO nanoparticles in HSQ and modifying surface chemistry, in order to enhance the performance of solar energy cells and flat panel displays.[8,9]

This work was partially supported by Ministry of Development and TUBITAK under the Project No. 110M412.

[1]J. Q. Xi, M. F. Schubert, J. K. Kim, E. F. Schubert, M. Chen, S. Y. Lin, W. Liu, and J. A. Smart, Nature Photon. **1**, 176 (2007).
[2]C. H. Sun, P. Jiang, and B. Jiang, Appl. Phys. Lett. **92**, 061112 (2008).
[3]A. Yildirim, H. Budunoglu, M. Yaman, M. O. Guler, and M. Bayindir, J. Mater. Chem. **21**, 14830 (2011).
[4]P. Vukusic and J. R. Sambles, Nature **424**, 852 (2003).
[5]A. R. Parker and H. E. Townley, Nat. Nanotechnol. **2**, 347 (2007).
[6]C. H. Sun, B. J. Ho, B. Jiang, and P. Jiang, Opt. Lett. **33**, 2224 (2008).
[7]C. Y. Park, J. M. Lim, J. S. Yu, and Y. T. Lee, Appl. Phys. Lett. **96**, 151909 (2010).
[8]X. T. Zhang, O. Sato, M. Taguchi, Y. Einaga, T. Murakami, and A. Fujishima, Chem. Mater. **17**, 696 (2005).
[9]K. Nakata, M. Sakai, T. Ochiai, T. Murakami, K. Takagi, and A. Fujishima, Langmuir **27**, 3275 (2011).
[10]T. Lohmüller, M. Helgert, M. Sunderman, R. Brunner, and J. P. Spatz, Nanolett. **8**, 1429 (2008).
[11]B. Paivanranta, P. K. Sahoo, E. Tocce, V. Auzelyte, Y. Ekinci, H. H. Solak, C. C. Liu, K. O. Stuen, P. F. Nealey, and C. David, ACS Nano **5**, 1860 (2011).
[12]K. Choi, S. H. Park, Y. M. Song, Y. T. Lee, C. K. Hwangbo, H. Yang, and H. S. Lee, Adv. Mater. **22**, 3713 (2010).
[13]H. Sai, H. Fujii, K. Arafune, Y. Ohshita, M. Yamaguchi, Y. Kanamori, and H. Yugami, Appl. Phys. Lett. **88**, 201116 (2006).
[14]Q. Chen, G. Hubbard, P. A. Shields, C. Liu, D. W. E. Allsopp, W. N. Wang, and S. Abbott, Appl. Phys. Lett. **94**, 263118 (2009).
[15]F. Buyukserin, M. Aryal, J. Gao, and W. Hu, Small **5**, 1632 (2009).